J Solid State Electrochem (2012) 16:2515–2521
DOI 10.1007/s10008-012-1663-1

ORIGINAL PAPER

Magneli phase Ti_nO_{2n-1} as corrosion-resistant PEM fuel cell catalyst support

Palanichamy Krishnan · Suresh G. Advani · Ajay K. Prasad

Received: 11 September 2011 / Accepted: 21 January 2012 / Published online: 16 February 2012

Abstract Magneli phase titanium suboxide, Ti_nO_{2n-1}, with Brunauer–Emmett–Teller surface area up to 25 $m^2\ g^{-1}$ was prepared using the heat treatment of titanium oxide (rutile) mixed with polyvinyl alcohol in ratios from 1:3 to 3:1. XRD patterns showed Ti_4O_7 as the major phase formed during the heat treatment process. The Ti_nO_{2n-1} showed excellent electrochemical stability in the potential range of −0.25 to 2.75 V vs. standard hydrogen electrode. The Ti_nO_{2n-1} was employed as a polymer electrolyte membrane fuel cell catalyst support to prepare 20 wt% platinum (Pt)/Ti_nO_{2n-1} catalyst. A fuel cell membrane electrode assembly was fabricated using the 20 wt% Pt/Ti_nO_{2n-1} catalyst, and its performance was evaluated using H_2/O_2 at 80 °C. A current density of 0.125 A cm^{-2} at 0.6 V was obtained at 80 °C.

Keywords Magneli phase titanium suboxide · PEM fuel cell · Catalyst support · Corrosion

Introduction

Polymer electrolyte membrane (PEM) fuel cells are considered as compact, quiet, and pollution-free power generation devices for various applications ranging from portable electronics to automotive propulsion. PEM fuel cell products are experiencing some commercial success in recent years [1, 2]. However, limited durability, high cost, and the lack of a hydrogen (H_2) supply infrastructure are some of the challenges that have slowed down the commercialization of PEM fuel cells. The U.S. Department of Energy has set fuel cell lifetime targets of 40,000 h for stationary power generation and 5,000 h for transportation applications, with less than 10% performance decay over their operating life. However, a lifetime of only around 2,500 h was reported for the transportation of PEM fuel cells in the year 2009 [3]. A major cause of limited lifetime is the degradation of fuel cell components. Hence, major advances in the development of novel fuel cell materials, especially the fuel cell electrodes, need to be achieved to meet the above targets.

Current commercial fuel cell electrodes are composed of noble metal catalysts such as platinum (Pt) supported on high surface area carbon supports such as Vulcan-XC-72. The carbon support enables the uniform dispersion of Pt nanoparticles, reduces their sintering or agglomeration over time, and provides electronic continuity. The cathode in the PEM fuel cell experiences a potential close to 1.0 V vs. standard hydrogen electrode (SHE) on contact with air under open-circuit conditions, i.e., when there is no current draw from the fuel cell. At such high potentials, the carbon support will undergo oxidation/corrosion, and the presence of Pt could further accelerate the corrosion [4]. The carbon corrosion leads to Pt agglomeration which leads to reduced electrochemically active catalyst surface area, loss of electronic continuity in the catalyst layer, and performance degradation. Hence, stable catalyst support materials that can withstand the high potentials in the PEM fuel cell need to be developed to improve the overall durability.

Development of corrosion-resistant PEM fuel cell catalyst supports is a very active research area in recent years [5–10]. Wang et al. [5] have reported that the durability of carbon nanotube-supported Pt catalyst is better than that of Vulcan-XC-72-supported Pt catalyst. However, extended durability of carbon nanotube-supported catalysts is yet to be studied, and

S. G. Advani · A. K. Prasad
Center for Fuel Cell Research,
Department of Mechanical Engineering,
University of Delaware,
Newark, DE, USA

P. Krishnan (✉)
Toda America Inc,
4750 W. Dickman Road,
Battlecreek, MI, USA
e-mail: krish10465@gmail.com

their high cost could also be an issue. Tungsten carbide [6] and conducting indium tin oxide [7] have also been investigated as alternative catalyst supports, but these are not very stable in the highly acidic environment that exists in the PEM fuel cell. Recently, Yin et al. [8] have investigated titanium diboride (TiB_2) as a stable Pt catalyst support material. They have reported that the stability of TiB_2-supported Pt catalyst is four times higher than that of Pt/C-supported catalyst. However, the DC electrical conductivity and fuel cell performance of TiB_2/Pt catalyst are not reported. Conducting polymers are also being considered as possible Pt catalyst supports. Polypyrrole [9] and polyaniline [10] have been used for this purpose, but the durability of conducting polymer-supported Pt catalysts needs to be studied in detail.

Many reports on the use of titanium oxide (TiO_2) as a corrosion-resistant Pt catalyst support are available in the literature [11–13]. Lim et al. [11] have sputtered Pt on Ti nanotube, and the catalyst is reported to be very stable, but the fuel cell performance is very low. Rajalakshmi et al. [12] have prepared Pt/TiO_2 catalyst and studied their fuel cell performance. They have reported that the durability of Pt/TiO_2 catalyst is better than that of Pt/C, but its higher electrical resistance could be due to the transition of TiO_2 from conducting to insulating state in the fuel cell environment. Huang et al. [13] have prepared a Pt/TiO_2 electrocatalyst by a template-assisted method; the catalyst exhibits excellent fuel cell performance as well as ultrahigh stability at high positive potentials.

Substoichiometric titanium oxides, Ti_nO_{2n-1}, known as Magneli phases, are extremely corrosion-resistant conducting oxides. The Magneli phases are prepared by heating the TiO_2 (rutile) under reduced atmosphere at 1,100 °C. The Magneli phase titanium oxides obtained from such heat treatment have good electrical conductivity and are highly resistant to various harsh chemical environments. They are being used as corrosion-resistant electrode materials in batteries and electrolyzers. Many studies on their use as a durable Pt catalyst support for fuel cell application have been reported [14–17]. They are extremely corrosion-resistant even at very high potential values. However, their low surface area of about 1–2 $m^2\ g^{-1}$ is the main disadvantage in preparing supported platinum catalysts with nanometer-scale particle size and good dispersion. Hence, suitable methods need to be developed to prepare substoichiometric titanium oxides, Ti_nO_{2n-1}, with high surface area. Toyoda et al. [18] have reported the preparation of high surface area Ti_nO_{2n-1} by the heat treatment of a mixture of TiO_2 (rutile) and polyvinyl alcohol (PVA) at 1,100 °C. The presence of PVA reduces the agglomeration of Ti_nO_{2n-1} resulting in high surface area. The aim of this paper is to exploit this method to prepare high surface area Ti_nO_{2n-1} and use it as a corrosion-resistant Pt catalyst support for PEM fuel cell application.

Experimental

Materials

Titanium oxide (rutile) 99.90%, polyvinyl alcohol 99.0%, sodium borohydride 99.0%, and 5 wt% Nafion solution, all from Sigma-Aldrich, USA, and chloroplatinic acid hexahydrate ($H_2PtCl_6{\cdot}6H_2O$) 99.90%, from Alfa-Aesar, USA, were used as received.

Preparation of Ti_nO_{2n-1}

The Magneli phase Ti_nO_{2n-1} with high surface area was prepared by a high temperature reduction process. The TiO_2 (rutile) was mixed with PVA in various proportions ranging from 25% to 75% PVA by weight. The mixture was homogenized using a mortar and pestle and transferred to ceramic boats, which were then placed inside a tubular furnace. The furnace was heated from room temperature to 1,100 °C at a heating rate of 3 °C/min under the atmosphere of 95% argon+5% hydrogen. The furnace temperature was maintained at 1,100 °C for 1 h and then cooled down to room temperature. The resulting Ti_nO_{2n-1} was ground using a mortar and pestle. The weight of Ti_nO_{2n-1} oxide obtained was about 90% of the weight of TiO_2 used for the preparation. The Ti_nO_{2n-1} prepared using 75% PVA and 25% TiO_2 by weight was used as the Pt catalyst support for further studies.

Characterization of Ti_nO_{2n-1}

The powder XRD patterns were recorded in the 2θ range 10–80° using a Rigaku D/Max-IIIC diffractometer with Cu Kα (λ=1.4518 Å) radiation filtered through Ni. The morphology of the powders was examined using a scanning electron microscope (SEM), JSM-7400 from JEOL Ltd., Japan. To examine the surface morphology, a pinch of the powder was adhered onto the SEM sample holder using a double-sided tape.

DC electrical conductivity of the prepared Ti_nO_{2n-1} samples was measured using a two-probe conductivity cell fabricated in our laboratory. The cell had a compartment with two copper foils for electrical contact. The compartment was filled with the Ti_nO_{2n-1} composite, the copper foils were assembled, and the cell was subjected to a constant pressure of 20 kg cm^{-2} in a hydraulic press. The voltage (V) of the terminal electrodes was scanned at a constant rate of 50 mV s^{-1} from 0 to 3.0 V, and the resulting current (I) was recorded. The electrical conductivity of the Ti_nO_{2n-1} composite was calculated from the slope of V vs. I plot.

The surface area of the Ti_nO_{2n-1} was determined using nitrogen adsorption–desorption isotherms at 77 K by the

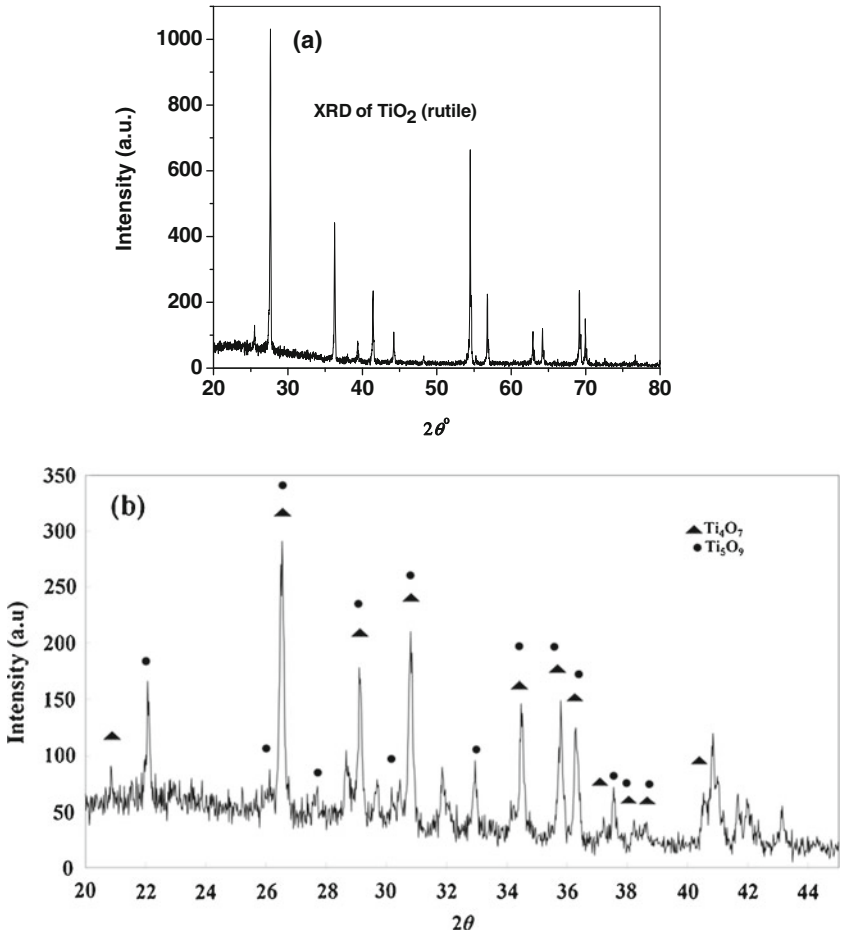

Fig. 1 X-ray diffraction pattern of **a** TiO_2 (rutile) and **b** Ti_nO_{2n-1} synthesized using 75 wt% PVA and 25 wt% TiO_2 (rutile)

Brunauer–Emmett–Teller (BET) method in a Micromeritics Accusorb 2100E apparatus. Prior to the measurements, the samples were maintained at 250 °C under vacuum for 8 h to eliminate adsorbed impurities.

Preparation of the Pt/Ti_nO_{2n-1} catalyst

The Ti_nO_{2n-1}-supported Pt catalyst was prepared by the sodium borohydride ($NaBH_4$) reduction method. Exactly 0.5 g of Ti_nO_{2n-1} was suspended in 25 ml of deionized water. Then, 0.318 g of $H_2PtCl_6{\cdot}6H_2O$ was added and sonicated for 1 h. Next, excess of 0.5 mol of $NaBH_4$ was added to the suspension under vigorous stirring. The mass was stirred for 30 m and filtered under suction; the Pt/Ti_nO_{2n-1} catalyst was washed with deionized water to completely remove the chloride. The Pt/Ti_nO_{2n-1} catalyst was dried overnight at 110 °C under vacuum and used for further studies. The Pt weight percent in the catalyst was determined by ICP-AES and found to be around 20 wt%.

Electrochemical stability studies

Electrochemical stability of the Ti_nO_{2n-1} catalyst support was studied by fabricating a standard Nafion-bonded microelectrode. Exactly 10 mg of Pt/Ti_nO_{2n-1} catalyst was suspended in 10 ml of isopropyl alcohol and sonicated for 30 m to prepare a suspension. Then, 10 μl of the suspension was dropped over a polished glassy carbon microelectrode, and the alcohol was allowed to evaporate. Next, 10 μl of 5 wt% Nafion suspension by weight was dropped over the catalyst to fix the catalyst to the glassy carbon microelectrode. Electrochemical stability of the catalyst was studied by cyclic voltammetry at a sweep rate of 50 mV s^{-1} using a VersaSTAT3 Potentiostat/Galvanostat from Princeton Applied Research, USA.

Fuel cell studies

Carbon paper (TGP-H-090) with 10 wt% Teflon coating from Toray, Japan, was used as the gas diffusion medium. Catalyst ink was prepared by mixing 20 wt% Pt/Ti_nO_{2n-1} catalyst and 5.0 wt% Nafion dispersion in the ratio of 65% catalyst and 35% Nafion by weight and stirred overnight with a magnetic stirrer. The ink was applied onto the Teflonized carbon paper using a camel-hair brush, and the carbon paper was mounted over a hot plate for solvent removal. The catalyst loading was controlled by periodic weighing of the catalyst-coated carbon paper to around 0.50 mg cm^{-2} of Pt.

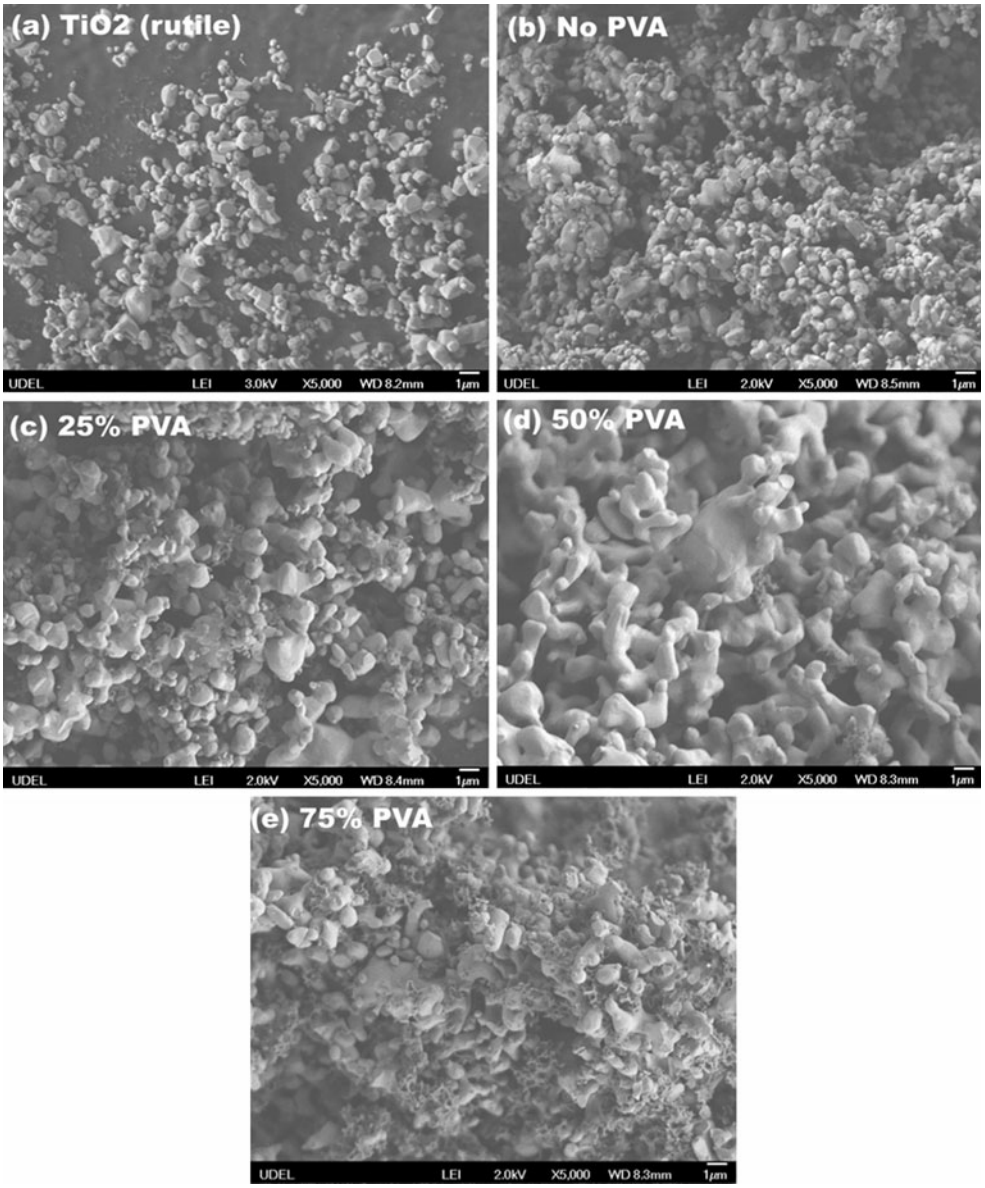

Fig. 2 SEM micrographs of **a** TiO_2 (rutile) and **b**–**e** Ti_nO_{2n-1} prepared using various ratios of TiO_2 (rutile) and PVA: **b** no PVA, **c** 25 wt% PVA, **d** 50 wt% PVA, and **e** 75 wt% PVA

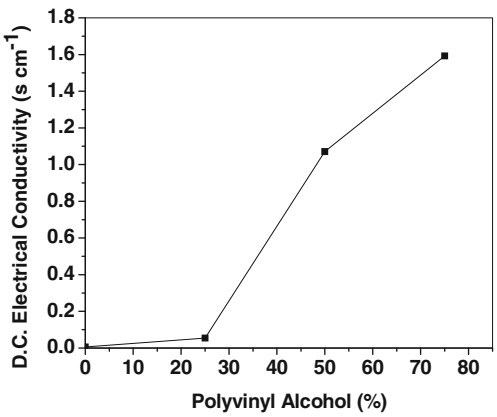

Fig. 3 DC electrical conductivity of Ti_nO_{2n-1} samples

The membrane electrode assembly (MEA) was fabricated by sandwiching a piece of Nafion 112 membrane between the two catalyst-coated gas diffusion electrodes and by hot pressing the assembly at 125 °C for 3 min under a pressure of 70 kg cm^{-2} using a laboratory hot press. The MEA was assembled in a 10-cm^2 fuel cell hardware, and its performance was evaluated with humidified H_2/O_2 gases at 80 °C using a fuel cell test station from Arbin Instruments, USA.

Results and discussion

The X-ray diffraction patterns of TiO_2 (rutile) and the Ti_nO_{2n-1} prepared with (75 wt% PVA) are shown in Fig. 1. The X-ray diffraction pattern of TiO_2 (rutile) matches with the diffraction pattern (JCPDS 88-1175) reported for

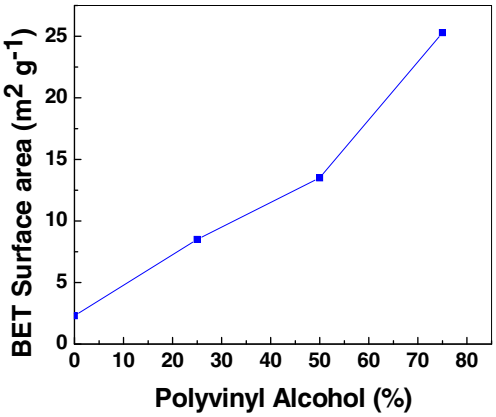

Fig. 4 BET surface area of Ti_nO_{2n-1} prepared using various ratios of TiO_2 (rutile) and PVA

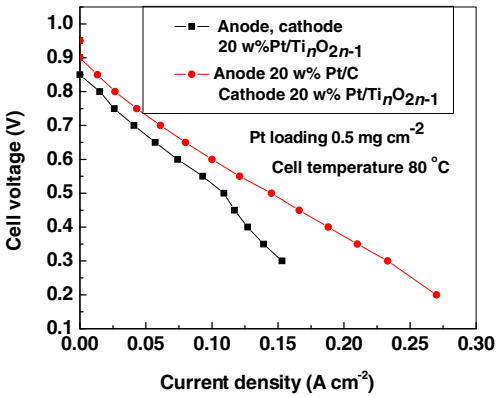

Fig. 6 Fuel cell performance of 20 wt% Pt/Ti_nO_{2n-1} catalyst

TiO_2 (rutile) in the literature [19]. The diffraction patterns of Ti_nO_{2n-1} were indexed as reported by Siracusano et al. [17]. The peaks of Ti_4O_7 (JCPDS 18-1402) and Ti_5O_9 (JCPDS 11-193) are indexed in Fig. 1b. The diffraction pattern exactly matches with that reported by Ioroi et al. [14] who assigned the diffraction peaks to a single phase of Ti_4O_7; a similar diffraction pattern in the present study confirms that Ti_4O_7 is the major Magneli phase oxide formed. We could not completely rule out the formation of other substoichiometric Ti_nO_{2n-1} oxides, such as Ti_5O_9, in very small proportions as we did observe many additional small diffraction peaks in the diffraction pattern.

SEM images of TiO_2 and the Ti_nO_{2n-1} prepared without adding PVA and with the addition of various percentages of PVA are shown in Fig. 2. The SEM images show interesting differences in the morphologies of TiO_2 and the Ti_nO_{2n-1} prepared with and without the addition of PVA. The TiO_2 particles are irregular in shape (Fig. 2a); the Ti_nO_{2n-1} prepared without adding PVA (Fig. 2b) comprises many spherical particles which appear dense and are agglomerated together resulting in low surface area. A majority of the particles look even smaller than the original TiO_2 particles.

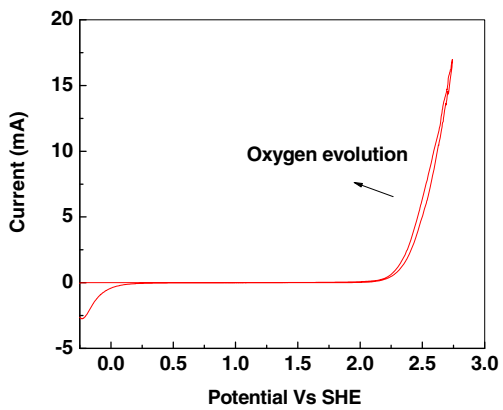

Fig. 5 Electrochemical stability of Ti_nO_{2n-1} in 0.5 M H_2SO_4

On adding 25% PVA by weight, the particle size has substantially increased (Fig. 2c), and the surface looks porous. On further increasing the PVA to 50 wt%, the particles resemble elongated rods with a porous nature (Fig. 2d). The particle agglomeration has substantially reduced with 75 wt% PVA (Fig. 2e). Similar observations have been reported in an earlier publication [18]. The SEM micrographs clearly demonstrate the changes in the morphology of Ti_nO_{2n-1} due to the addition of various amounts of PVA during the heat treatment process. However, the morphology of the Ti_nO_{2n-1} samples prepared in this study is somewhat different from that of [18]. The difference could be mainly due to the different gas environments employed in the two studies despite maintaining the same furnace temperature. Toyoda et al. [18] have passed nitrogen gas through the furnace; whereas in the present study, a mixture of argon (95%) and hydrogen (5%) was passed through the furnace. The pyrolysis products of PVA in the present study will be different from that of [18], due to the use of H_2 in our furnace. In the presence of H_2, oxygen in the pyrolysis products of PVA will be converted into water resulting in the generation of more hydrocarbons. The more reducing furnace conditions in the present study could be the reason for the difference between the morphology of the Ti_nO_{2n-1} prepared in the present study and in [18].

DC electrical conductivity of the Ti_nO_{2n-1} oxides prepared in this study is plotted in Fig. 3. The conductivity of Ti_nO_{2n-1} oxide prepared without the addition of PVA was 5.75 mS cm^{-1}. The conductivity of Ti_nO_{2n-1} oxide increased with an increase in the percentage of PVA, and a maximum conductivity of 1.59 S cm^{-1} was obtained with the Ti_nO_{2n-1} sample prepared with 75 wt% PVA. The increase in the conductivity of the Ti_nO_{2n-1} oxides with an increase in the PVA content shows that the carbon coating on the surface of the Ti_nO_{2n-1} could contribute towards the increase in the conductivity of the Ti_nO_{2n-1} oxides. DC electrical conductivity in the range of 150–1,000 S cm^{-1} has been reported for the Magneli phase Ti_nO_{2n-1} oxides [20].

The conductivity values of the Ti_nO_{2n-1} oxides prepared in this study are lower than that reported in the literature. The reason for the low conductivity of the Ti_nO_{2n-1} oxides prepared in this study is not clear.

The increase in the BET surface area with increasing PVA content is plotted in Fig. 4. Ti_nO_{2n-1} prepared without PVA has a very low surface area of 2.14 $m^2\ g^{-1}$. Many publications have reported BET surface areas of 1 to 2 $m^2\ g^{-1}$ for the Magneli phase Ti_nO_{2n-1} oxides [14–17]. The low surface area is mainly due to particle sintering as a result of the very high temperature (1,100 °C) during the heat treatment process. The BET surface area of Ti_nO_{2n-1} increases with the addition of PVA before the heat treatment process. BET surface areas of 13.50 and 25.30 $m^2\ g^{-1}$ were obtained for the Ti_nO_{2n-1} samples prepared with 50 and 75 wt% PVA, respectively. It has been reported that PVA addition results in the coating of the Ti_nO_{2n-1} with a thin layer of carbon that reduces particle agglomeration and increases its surface area [18]. It can be seen from the SEM micrographs (Fig. 2) that the Ti_nO_{2n-1} samples prepared with 25 and 50 wt% PVA have particles that are in fact bigger than those of the Ti_nO_{2n-1} prepared without PVA. The increased surface area of the Ti_nO_{2n-1} samples prepared with 25 and 50 wt% PVA is due to the porous carbon coating and the change in the particle morphology. Particle sintering has noticeably reduced for the Ti_nO_{2n-1} prepared with 75 wt% PVA (Fig. 2e). The Ti_nO_{2n-1} samples may contain some quantity of carbon due to the decomposition of PVA. The final weight of the Ti_nO_{2n-1} obtained in all these experiments was about 90% of the initial weight of TiO_2 showing that the free carbon, if present, is negligible. Hence, the increase in the BET surface area is mainly due to the porous nature of the surface due to carbon coating and the reduction of particle agglomeration.

Electrochemical stability of Ti_nO_{2n-1} in 0.50 M sulfuric acid (H_2SO_4) in the potential range of −0.2 to 2.75 V vs. SHE is shown in Fig. 5. It can be seen that the Ti_nO_{2n-1} is extremely corrosion-resistant; no oxidation peaks appear until the potential reaches about 2.25 V vs. SHE. The oxidation peak beyond 2.25 V is due to oxygen evolution, and reduction peaks at potentials below −0.2 V could be due to either the reduction of titanium oxides or hydrogen evolution [16]. The corrosion resistance behavior of Magneli phase titanium oxides is well known and they are increasingly being used as catalyst supports in solid polymer electrolyzers and in fuel cells [16, 17].

The corrosion stability of Pt/Ti_nO_{2n-1} was compared with the commercial Pt/Vulcan-XC-72-supported catalyst by maintaining at various voltages up to 1.5 V. The Pt/Ti_nO_{2n-1} catalyst was quite stable even after maintaining at 1.50 V, whereas the catalytic activity of Pt/Vulcan-XC-72 substantially reduced due to the carbon corrosion at high voltages [15].

The fuel cell performance of the Pt/Ti_nO_{2n-1} catalyst is shown in Fig. 6. The open-circuit voltage was around 1.0 V, but the voltage quickly dropped on applying a load, and the cell could provide only about 0.125 $A\,cm^{-2}$ at 0.6 V which is very low when compared with the state-of-the-art membrane electrode assemblies. The low performance is mainly due to the low conductivity of the Ti_nO_{2n-1} prepared in this study, and the difficulty in preparing a homogenous catalyst ink with the Pt/Ti_nO_{2n-1} catalyst is probably due to the large particle size of the Ti_nO_{2n-1} support. Size reduction of the Ti_nO_{2n-1} support by suitable methods and modification of the solvent composition in the catalyst ink may improve the performance of the MEA. This work has demonstrated the preparation of Ti_nO_{2n-1} oxides with high surface area by using PVA during the heat treatment process. However, further studies to improve the DC electrical conductivity of the Ti_nO_{2n-1} are required in order to improve the fuel cell performance.

Conclusions

Magneli phase Ti_nO_{2n-1} with high surface area (25 $m^2\ g^{-1}$) was prepared by the heat treatment of TiO_2 (rutile) with various percentages of polyvinyl alcohol. The prepared oxide shows Ti_4O_7 as the predominant phase. The DC electrical conductivity of the Ti_nO_{2n-1} oxides was somewhat low in the range of 0.057–1.59 $S\,cm^{-1}$. The Ti_nO_{2n-1} shows excellent electrochemical stability in the potential range of −0.25 to 2.75 V vs. SHE. The fuel cell performance of 20 wt% Pt/Ti_nO_{2n-1} was measured at 80 °C using humidified H_2/O_2 and found to be rather low (around 0.125 $A\,cm^{-2}$ at 0.6 V). The low fuel cell performance is due to the low electrical conductivity of the Ti_nO_{2n-1} and the difficulty in preparing a homogenous catalyst ink. Further studies are needed to improve the fuel cell performance of corrosion-resistant Pt/Ti_nO_{2n-1} catalysts.

Acknowledgment The work was supported by the Federal Transit Administration.

References

1. Yan WM, Wang XD, Lee DJ, Zhang XX, Guo YF, Su A (2011) Appl Energ 88:392–396
2. Frenette G, Forthoffer D (2009) Int J Hydrog Energ 34:3578–3588
3. Wang Y, Chen KS, Mishler J, Cho SC, Adroher XC (2011) Appl Energ 88:981–1007
4. Roen LM, Paik CH, Jarvic TD (2004) Electrochem Solid St 7: A19–A22
5. Wang X, Li W, Chen Z, Waje M, Yan Y (2006) J Power Sources 158:154–159
6. Zellner MB, Chen JGG (2005) Catal Today 99:299–307

7. Chhina H, Campbell S, Kesler O (2006) J Power Sources 161:893–900
8. Yin S, Mu S, Lv H, Cheng N, Pan M, Fu Z (2010) Appl Catal B-Environ 93:233–240
9. Huang SY, Ganesan P, Popov BN (2009) Appl Catal B-Environ 93:75–81
10. Kim S, Park SJ (2008) Solid State Ionics 178:1915–1921
11. Lim DH, Lee WJ, Macy NL, Smyrl WH (2009) Electrochem Solid St 12:B123–B125
12. Rajalakshmi N, Lakshmi N, Dhathathreyan KS (2008) Int J Hydrog Energ 33:7521–7526
13. Huang SY, Ganesan P, Popov BN (2010) Appl Catal B-Environ 96:224–231
14. Ioroi T, Siroma Z, Fujiwara N, Yamazaki S, Yasud K (2005) Electrochem Commun 7:183–188
15. Ioroi T, Senoh H, Yamazaki SI, Siroma Z, Fujiwara N, Yasuda K (2008) J Electrochem Soc 155:B321–B326
16. Walsh FC, Wills RGA (2010) Electrochim Acta 55:6342–6351
17. Siracusano S, Baglio V, D'Urso C, Antonucci V, Aricò AS (2009) Electrochim Acta 54:6292–6299
18. Toyoda M, Yano T, Tryba B, Mozia S, Tsumura T, Inagaki M (2009) Appl Catal B-Environ 88:160–164
19. Samuel V, Muthukumar P, Gaikwad SP, Dhage SR, Ravi V (2004) Mater Lett 58:2514–2516
20. Gusev AA, Avvakumov EG, Medvedev AZH, Masliy AI (2004) Chem Sust Dev 12:313–318